INTERNATIONAL JOURNAL OF EXPLORING EMERGING TRENDS IN ENGINEERING
Peer-Reviewed, Refereed, Indexed and International Journal, https://ijoeete.com/
|ISSN No. 2394-0573 |Volume: 1, Issue: 01 | July - Dec 2023

PLANT LATEX MEDIATED GREEN SYNTHESIS OF CeO_2 NANOPARTICLES FOR LUMINESCENCE AND PHOTOCATALYTIC STUDIES

Sreenivasan N.S.[a] , L.S. Reddy Yadav[b], R. Venkatesh [c],N. Dhananjaya[c] Satyavir Singh[d]

[a]Department of Chemistry, KNS Institute of Technology, Bangalore-560064, India
[b]Department of Chemistry, BMS Institute of Technology & Management, Bangalore-560064, India
[c]Department of Physics, BMS Institute of Technology & Management, Bangalore-560064, India
[a]Department of Chemistry, Arunodaya University, Itanagar, Arunchal Pradesh-791110,India.

Abstract:
CeO2 nanoparticles were produced in this prior study using latex extracted from the E. Tirucalli plant. Analytical methods such as PXRD, PL, SEM, and TEM were used to investigate the nanoparticles of CeO2 that were produced and determine their structure and appearance. The XRD signal shows that the crystal structure of the produced chemical is that of cubic fluorite. CeO2 powder's particle size was measured using the Scherer formula, and it was determined to be between 14 nm and 30 nm. CeO2 nanoparticles appeared in SEM micrographs as aggregated, puffy, and plate-like clusters. TEM analysis of CeO2 nanoparticles reveals that they are 10 nm in size and have an ellipsoid or spherical shape. Photoluminescence (PL) tests were also performed on the CeO2 nanoparticles. The oxygen-related flaws in CeO2 nanoparticles account for the PL emission peak seen at 237 nm excitation. The photocatalytic activity may be attributed to the CeO2 nanoparticles.

Keywords: *E. Tirucalli*; Green synthesis; CeO_2 nanoparticles; SEM; TEM.
Corresponding author:

Introduction:
The lattice constant of the cubic fluorite crystal structure of CeO2 is a = 0.541 nm. Possible uses include ion guiding layers, an optical covering, and ideal buffer layers for creating epitaxial formed functional oxides on silicon substrata [1-4] , thanks to its optical photograph, thermal and chemical constancy, high refractive index, and high dielectric constant. It was found to be an excellent metal oxide with variable emission peaks of various shapes and sizes. Few papers on CeO2's photoluminescence characteristics have been published so far [5-7]. CeO2 nanoparticles are of great interest because of the wide range of uses to which they may be put, including in sun protection products, solid electrolytes, refining mediators, solar cells, fuel cells, oxygen pumps, phosphor/luminescence, photocatalysis, sensors, and metallurgy. Cerium's strong thermodynamic attraction for oxygen and sulphur, its potential redox chemistry consisting of Ce3+/Ce4+, and the existence of solely favourable absorption/excitation energy peaks associated to its electronic structure [8-11] all contribute to the success of these applications.
The elimination of carcinogenic dyes in wastewater treatment is a growing topic of study due to the widespread use of synthetic colours in everyday life. Therefore, a cost-effective and efficient technique of degrading this extremely carcinogenic dye is being sought. Because the reactions occur under renewable solar energy that is both cheap and easy to utilise, photocatalytic degradation of dyes using UV/sun light is one of the most popular ways. [12-16].
An accepted green synthesis method is one that can be used in a variety of contexts and requires little resources to implement. [17-20].
The latex of the E. Tirucalli plant was used in the synthesis of CeO2 nanoparticles for this study. There was much research into and discussion of the luminescence and structural features.

Synthesis of CeO_2 nanoparticles:
CeO2 nanoparticles were synthesised using latex extracted from the E. Tirucalli plant [21]. For this CeO2 synthesis, 2 grammes of Ce (NO3)3. 6H2O were dissolved in 10 millilitres of distilled water [22], and then 5 millilitres of E. Tirucalli plant latex were added to the mixture. After 5-10 minutes of vigorous stirring with a magnetic stirrer, the reaction mixture was transferred to a muffle furnace warmed to 350 10 oC. Foam is produced as a byproduct of thermal dehydration in the reaction mixture. It just took a few minutes to complete the operation. The final product was calcined at 900 degrees Celsius for three hours to remove impurities before being put to scientific use.

Results and discussions

Structural characterization (PXRD)

INTERNATIONAL JOURNAL OF EXPLORING EMERGING TRENDS IN ENGINEERING
Peer-Reviewed, Refereed, Indexed and International Journal, https://ijoeete.com/
|ISSN No. 2394-0573 |Volume: 1, Issue: 01 | July - Dec 2023

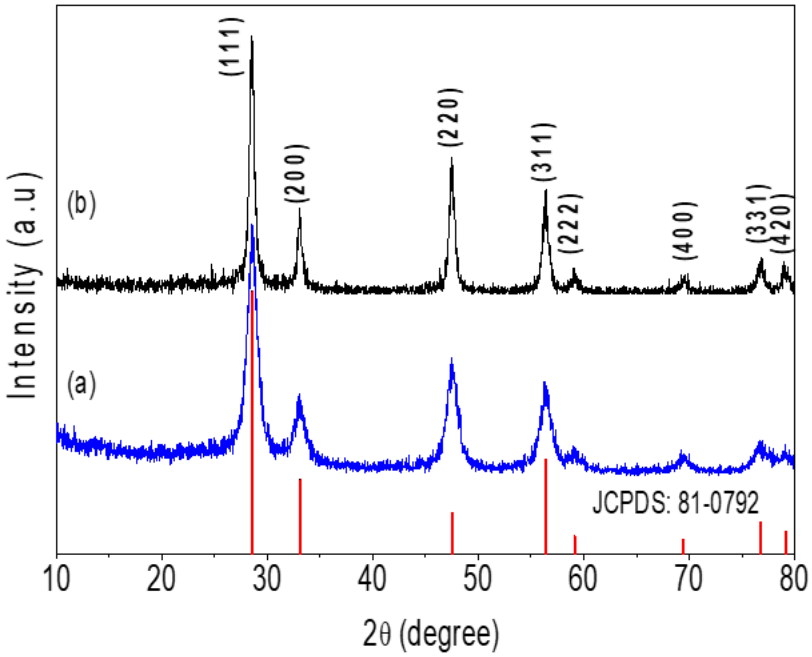

Fig.1. PXRD patterns of CeO2 nanoparticles (a) as-formed and (b) calcined at 900 °C for 3 hours.

CeO2 nanoparticles, both as-formed and calcined at 900 °C for 3 hours, are shown in PXRD in Fig. 1. The planes (111), (200), (220), (311), (222), (400), (331), and (420) all exhibit a steep peak at 2 = 28.5, 33.1, 47.5, 56.3, 59.1, 69.4, 76.7, and 79.1. These peaks may be mapped to the known three-dimensional structure of the face-centered cubic phase (JCPDS cards no. 81-0792). The absence of any additional impurity-related peak was observed [23]. Scherrer's formula was also used to determine that the average particle size of CeO2 powder is between 14 nm and 30 nm. The famous Debye-Scherrer

$$D = \frac{0.9\,\lambda}{B \cos\theta}$$

Where D is the crystal diameter, t the FWHM of the diffraction peak, and the scattering angle.

SEM and TEM morphology analyses

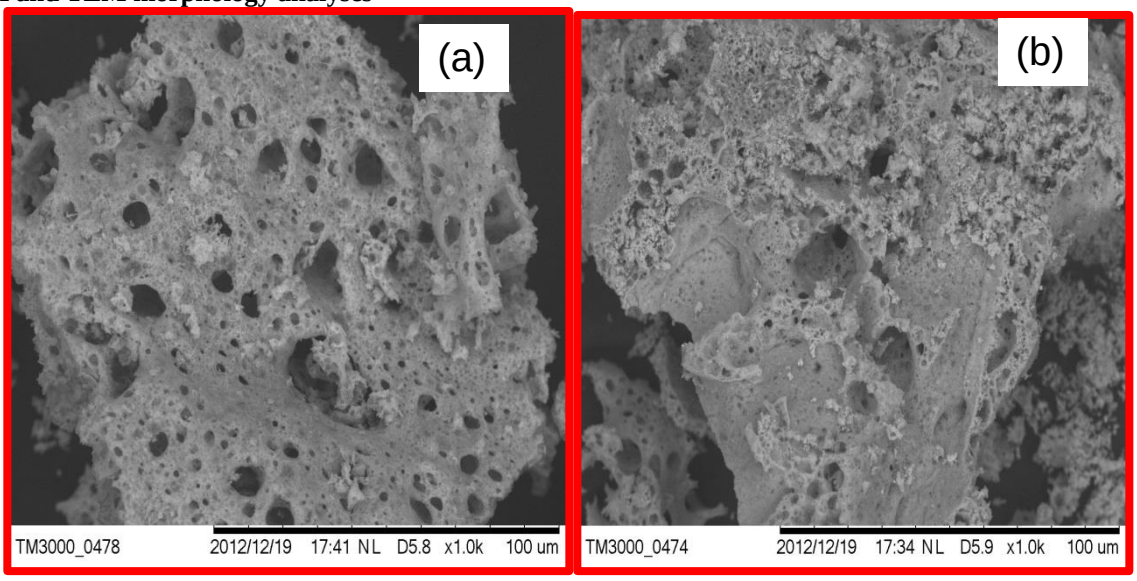

INTERNATIONAL JOURNAL OF EXPLORING EMERGING TRENDS IN ENGINEERING
Peer-Reviewed, Refereed, Indexed and International Journal, https://ijoeete.com/
|ISSN No. 2394-0573 |Volume: 1, Issue: 01 | July - Dec 2023

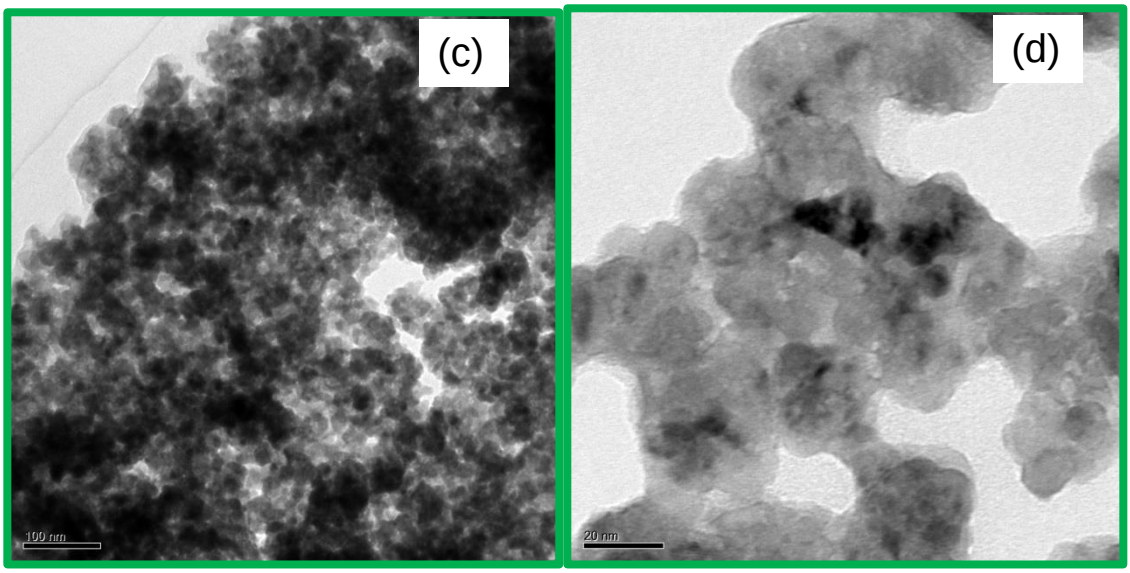

Fig. 2. Nanoparticles of CeO2 (a) and (c) as-formed in a SEM and TEM; (b) and (d) after being calcined at 900 °C for 3 hours

SEM micrographs of as-formed and 900 C for 3 h calcined CeO2 nanoparticles are shown in Figure 2(a) and (b), respectively. As they developed, the nanoparticles were agglomerated into larger, porous structures of several microns in size. It has been widely reported that clumping nanoparticles together may reduce their surface free energy. Large quantities of gases were generated during combustion synthesis, which led to the presence of gaps and voids in the sample [8]. Fig.2. (c) displays TEM images that were used to examine the particle size of the CeO2 powder. When compared to Scherrer's approach [24-26], the morphology of the CeO2 nanoparticles was consistent, with well-distributed elliptical/spherical particles having an average size of 10 nm (Fig. 2. (d)).

Photoluminescence (PL) study

In Fig. 3 we can see the PL spectrum of a nanoparticle of cubic CeO2 stimulated at 237 nm. Below the excitation of 235 nm, we observed a faint emission peak at 420 nm and well-defined emission peaks at 393, 484, 530, and 600 nm. Surface defects in CeO2 nanoparticles are characterised by a wide emission peak at 393 nm, a blue emission peak at 420 nm, a blue-green peak at 483 nm, a faint green peak at 530 nm, and a red emission peak at 600 nm. The strongest peak may be associated with the 393 nm transitions between 5d and 2F5/2 and 5d and 2F7/2. Many studies [10] examined PL of CeO2 nanoparticles with altered particle size and shape, and their findings were quite comparable to those presented here. CeO2 with a particle size of 2 nm was synthesised, and its blue emission peaked at 425 nm (2.92 eV), with further peaks at 405 nm (389 nm), and 368 nm (violet/blue light) [10]. Furthermore, in rod and flower-like, there were three (370, 414, and 468 nm) and two (415, 435 nm) emission peaks, respectively [27-30].

INTERNATIONAL JOURNAL OF EXPLORING EMERGING TRENDS IN ENGINEERING
Peer-Reviewed, Refereed, Indexed and International Journal, https://ijoeete.com/
|ISSN No. 2394-0573 |Volume: 1, Issue: 01 | July - Dec 2023

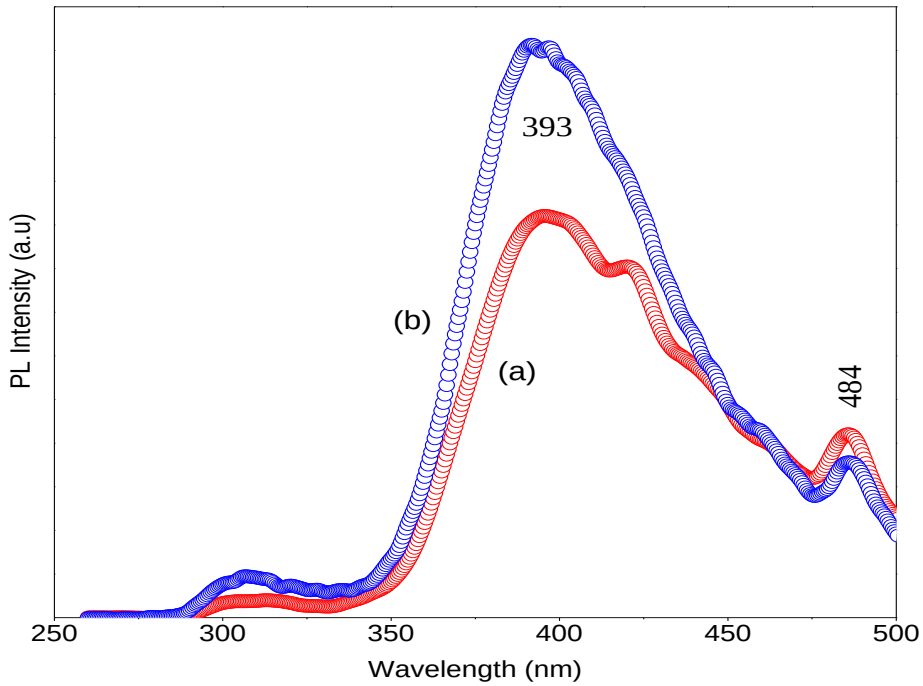

Fig. 3. PL spectra under 237 nm excitation of (a) as-formed CeO2 nanoparticles and (b) 900 C for 3 h calcined CeO2 nanoparticles with 5 ml, esterase's included E. Tirucalli plant latex.

CeO2 nanoparticles' photocatalytic properties.
Under UV - light and solar light sources, photocatalytic activity for the CeO2 Nps was tested by degrading MB dye at varied catalytic doses, effects of pH, dye concentrations, and other factors [31-33].
Result of catalytic dosage

Experiments were carried out to investigate what would happen if varying amounts of catalyst ranging from 50 to 200 mg were added to 100 millilitres of MB dye solution with a pH of 7. The findings that were obtained are shown in Figure 4. In each scenario, increasing the amount of catalyst used resulted in a higher rate of deterioration occurring per unit of time. However, the effectiveness of UV radiation is higher than that of solar sunlight and and arise in the amount of catalyst has no impact on the rate at which the dye degrades [34–37].

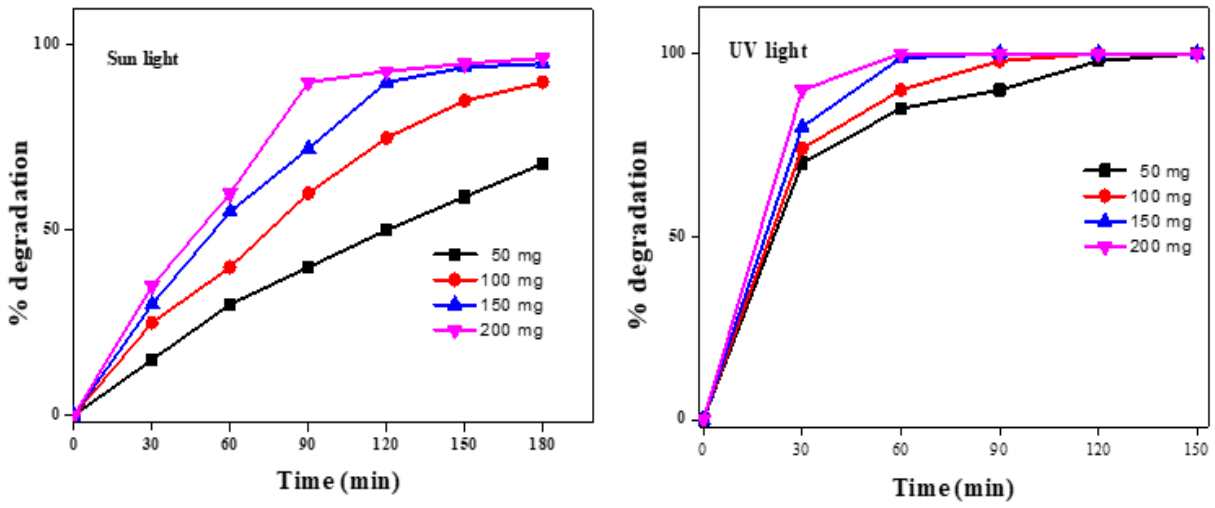

Fig. 4 The effect of UV and solar radiation on catalytic dosage.

Result of pH vary:
Figure 5 provides a graphical representation of the influence that pH has on the disintegration of MB dye. It is

INTERNATIONAL JOURNAL OF EXPLORING EMERGING TRENDS IN ENGINEERING
Peer-Reviewed, Refereed, Indexed and International Journal, https://ijoeete.com/
|ISSN No. 2394-0573 |Volume: 1, Issue: 01 | July - Dec 2023

currently shown that acidic environments are less favourable for deteriorating ability than basic conditions [38–43]. In addition, this helps achieve better colour separation. At higher pH levels, a greater concentration of hydroxyl radicals that catalysed degradation was discovered. At pH 9, more degradation was seen in both scenarios; however, the capability of UV light was more comprehensive when compared to that of solar radiation.

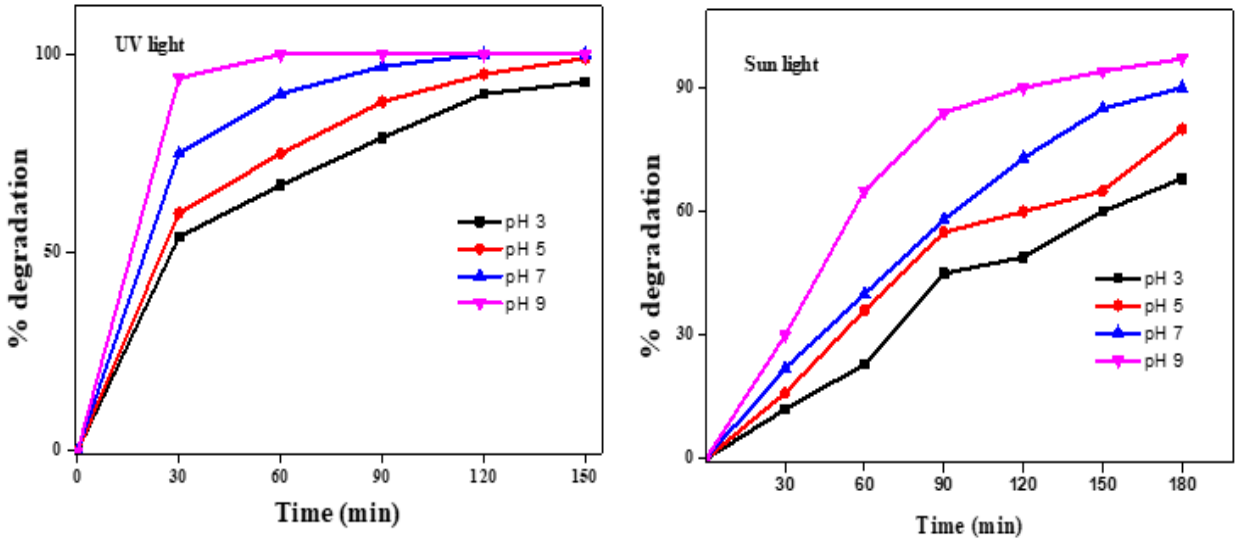

Fig.5. The impact of sunlight and ultraviolet light on pH.

Result of dye concentration

Figure 6 provides a visual representation of the effect that the dye concentration has on the MB dye's rate of degradation. During the course of the studies, the concentration of MB dye ranged from 5 to 20 g/ml, the quantity of catalyst was 100 mg/100 ml, and the pH was 7. Because the presence of a greater number of dye molecules on the surface of the catalyst results in a decreased number of active sites that are accessible for degradation, the concentration of the dye has a negative impact on the efficiency of the degradation process [44–49].

Result of UV light and sun light

An examination of the rate of MB dye deterioration in a 20 ppm solution under two unique illumination conditions was presented to us in Figure 7. It was hypothesised that exposure to UV radiation, such as that seen in sunlight, would cause the MB dye to degrade very rapidly. In the visible range, CeO2 exhibits a band gap that is either on par with or even larger than its band gap in the ultraviolet area. Because of this, they are beneficial to the process of photocatalysis that is generated by ultraviolet light [50, 51].

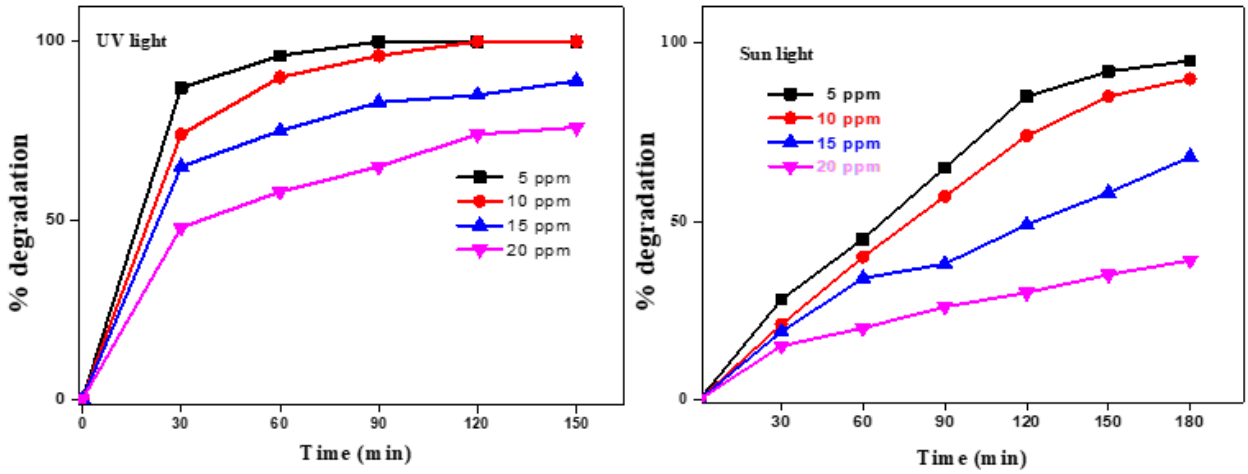

Fig .6. Result of dye concentration under UV-light and sun light.

INTERNATIONAL JOURNAL OF EXPLORING EMERGING TRENDS IN ENGINEERING
Peer-Reviewed, Refereed, Indexed and International Journal, https://ijoeete.com/
|ISSN No. 2394-0573 |Volume: 1, Issue: 01 | July - Dec 2023

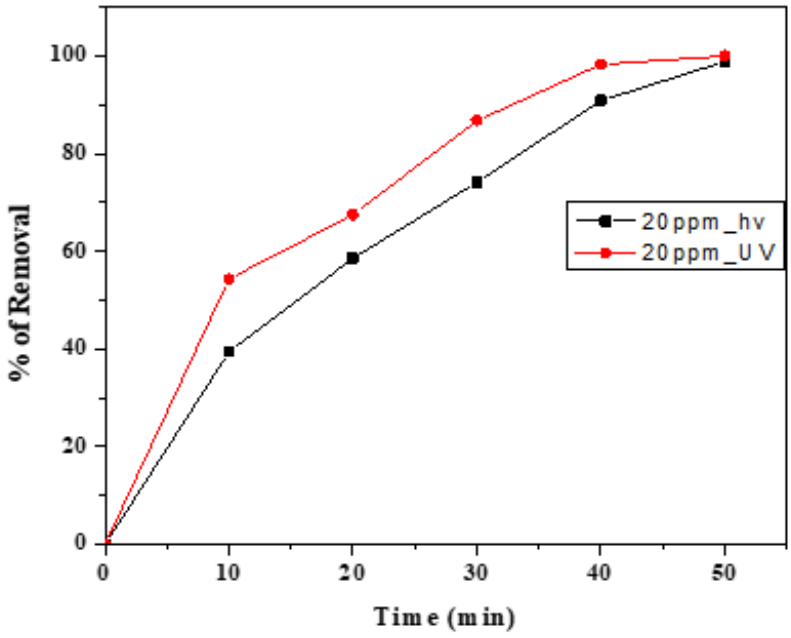

Fig. 7. Sunlight and UV rays cause 20 ppm of MB to degrade over time.

Conclusions

We were able to effectively synthesise CeO2 nanoparticles by using the latex of the E. Tirucalli plant as the fuel in a procedure that involves environmentally friendly burning. According to the results of the PXRD experiments, the crystal structure was entirely cubic. The formula developed by Scherrer made it possible to provide an accurate estimate of the particle size. As can be seen in the micrographs that were obtained by the SEM, the plant latex from the E. tirucalli species was shown to be very effective in controlling the shape and size of the CeO2 nanoparticles. Beginning at a wavelength of 237 nm, the photoluminescence (PL) spectrum of a CeO2 nanoparticle displays well defined emission peaks at about 393 nm, 484 nm, 530 nm, and 600 nm.

References

1. C. B. Murray, C.R. Kagan, Annu Rev Mater Sci. **30,** 545 (2000).
2. P. Ramesh, A. Rajendran, M. Meenakshi Sundaram, J. of Nano sci and nano tech. **2,** 41 (2014).
3. K. Manjunath, T. Ramakrishnappa, G. Nagaraju, Ionics. **23,** 2887 (2017).
4. T. F. Ma, J. Bai, and C. P. Li, Vacuum. **145,** 47 (2017).
5. C. Su, J. Li, Q. Zhu, J Appl Cat A: General. 202, 81 (2000).
6. A. Muthuvel, M. Jothibas, C. Manoharan, Nanotech for Environ Engg, 5, 14 (2020).
7. A. Muthuvel, M. Jothibas, C.Manoharan, J. of Env. Chem Engg. 8, 103705 (2020).
8. Nabil Al-Zaqri, A. Muthuvel, M. Jothibas, Ali Alsalme, Fahad A.Alharthi, V. Mohan, Inorg. Chem Comm.127, 108507 (2021).
9. K. Mamjunath, T. Jayalakshmi, G. Nagaraju, J. Mater Res Technol. **7,** 7 (2018).
10. N. F. Jaafar, A. A. Jalil, S. Triwahyono, M. N. M. Muhid, N. Sapawe, and M. A. H. Satar, Chem. Eng. Jour. **191,** 112 (2012).
11. L.S. Reddy Yadav, M. Raghavendra, G. Nagaraju, T. Ramakrishnappa, Curr. Nano Mater. **4,** 223 (2019).
12. R. Mahtab, J.P. Rogers, J Am Chem Soc. **117,** 9099 (1995).
13. L.S. Reddy Yadav, K. Manjunath, G. Nagaraju, J.of Sci: Adv, Mate. and Dev. **3,** 181 (2018).
14. R.L. Edelstein, M. M. Miller, Biosensors Bioelectron. **14,** 805 (2000).
15. A. Syed, L.S. Reddy Yadav, G. Nagaraju, Crystals. **10,** 0817 (2020).
16. M. Bruchez, M. Moronne, Science. **281,** 2013 (1998).
17. W.C. W. Chan, S. M. Nie, Science**. 281,** 2016 (1998).
18. S. Pratibha, N. Dhananjaya, J. of Mat.Sci: Mater. in Electr. **30,** 6745 (2019).
19. A. de la Isla, W. Brostow, B. Bujard, Mat Resr Innovat. **7,** 110 (2003).
20. J. Ma, H.Wong, Nanotechnology. **14,** 619 (2003).
21. R.S. Molday, D. MacKenzie, J Immunol Methods. **52,** 353 (1982)

22. L.S. Reddy Yadav, N. Dhananjaya, K.H. Sudheer Kumar, J.of Sci: Adv, mat. Dev. **3,** 303 (2018).
23. G. Busca, Elsevier, New York,, USA, (2014).
24. D. Ciuparu, A. Ensuque, G. Shafeev, F. Bozon-Verduraz, J. of Mater.Sci. **19,** 931 (2000).
25. C. Suciu, L. Gagea, A.C. Hoffmann and M. Mocean, Chem. Eng. Sci. **61**, 7831 (2006).
26. O. Vasylkiv, Y. Sakka, J Am Ceram Soc. 84, 2489 (2001).
27. L.S. Reddy Yadav, N. Dhananjaya, K.H. Sudheer Kumar, G. Nagaraju, Eur. Phys. J. Plus. **133,** 153 (2018).
28. M. Mazaheri, M. Valefi, M. RazaviHesabi, J Ceram Int. **35,** 13 (2007).
29. L.S. Reddy Yadav, N. Dhananjaya, K.H. Sudheer Kumar, Eur. Phys. J. Plus. **131,** 7 (2016).
30. M.T. Taghizadeh, M. Vatanparast, J Colloid Interface Sci. **483,** 1 (2016).
31. A. Khataee, B. Kayan, P. Gholami, D. Kalderis, S. Akay, L. Dinpazhoh, Ultra sonics Sono chemist. **39,** 540 (2017).
32. F. Heshmatpour, R.B. Aghakhanpour, Powder Technol. **205,** 193 (2011).
33. A. Babaei, M. Babazadeh, H.R. Momeni, Int. J. Electrochem. Sci. **6,** 1382 (2011).
34. P. Norouzi, M.P. Hamedani, M.R. Ganjali, F. Faridbod, Int. J. Electrochem. Sci. **5,** 1434 (2010).
35. D. Kumar, H. Nagabhushana, G. Nagarju, AIP Conf. proceed. **1665,** 050145 (2015).
36. K. Yeragani, M. Tancer, P. Chokka, G. B. Baker, A. Carlsson, Indian J. Psychiatr. **52,** 87 (2010).
37. R. Venkatesh, N. Dhananjaya, M. K. Sateesh, J.P, Shabaaz Begum, S.R. Yashodha. H. Nagabhushana, C. Shivakumara, J, of Alloys and Comp. **732,** 725 (2018).
38. D. V. Pinjari, K. Prasad, and P. R. Gogate, Chem.Eng. and Pro. **74,** 178 (2013).
39. L.S. Reddy Yadav, N. Dhananjaya, S. Pratibha, G. Nagaraju, J. of Sci: Adv. Mater. dev. **4,** 425 (2019).
40. L. S. Reddy yadav, R. Venkatesh, M. Raghavendra, T. Ramakrishnappa, N.Dhananjaya, G. Nagaraju, Curr. Nanomater. **5,** 66 (2020).
41. C. Kontoyannis, M. Orkoula, J. Mater. Sci. **29,** 5316 (1994).
42. D. A. Ward, E.I. Ko, Chem. Mater. **5,** 956 (1993).
43. M.W. Pitcher, S.V. Ushakov, A. Navrotsky, B.F Woodfield, G. Li, J. Am. Ceram. Soc. **88,** 160 (2005).
44. L.S. Reddy Yadav, S. Rajesh, J. Nanostru. **6,** 250 (2016).
45. L. S. Reddy Yadav, K. Lingaraju, C.Kavitha, H. Nagabhushana, G.Nagaraju, Int. J. of Nanosci. **15,** 155 (2015).
46. L.S. Reddy Yadav, K. Manjunath, B. Archana, H. Raja Naika, H. Nagabhushana, G. Nagaraju, Eur. Phys. J. Plus. **131,**154 (2016).
47. L.S. Reddy Yadav, H. Raja Naika, H. Nagabhushana, G. Nagaraju, Int. J; of Nanosc. **15,** 1550033 (2015).
48. L. S. Reddy Yadav, C. Kavitha, G. Nagaraju, Eur. Phys. J. Plus. **132,** 239 (2017).
49. L.S. Reddy Yadav, K. Manjunath, G. Nagaraju, J.of Mater. Sci: Mat. in Electr. **29,** 8747
50. L. S. Reddy Yadav, K. Manjunath, G.K. Raghu, G. Nagaraju, Mat. Res. Exp. **4,** 28 (2017).
51. L.S. Reddy Yadav, K. Manjunath, B. Archana, H. Raja Naika, H. Nagabhushana, G. Nagaraju, Inter. J. of Nanosci. **15,** 1650013 (2016).